


Adsorptive separation of Pb(II) and Cu(II) from aqueous solutions using as-prepared carboxymethylated waste Lyocell fiber

J. K. Bediako¹ · S. Kim¹ · W. Wei¹ · Y.-S. Yun¹ 

Received: 2 September 2015 / Revised: 6 November 2015 / Accepted: 14 December 2015 / Published online: 11 January 2016
© Islamic Azad University (IAU) 2016

Abstract Adsorptive separation of Pb(II) and Cu(II) using modified waste Lyocell fiber adsorbent was investigated in this research. The waste Lyocell fiber was functionalized through carboxymethylation of the hydroxyl moieties using sodium chloroacetate as modifying agent and was crosslinked with epichlorohydrin to provide water stability. The maximum equilibrium batch uptake in single metal system was 353.45 mg/g for Pb(II) and 98.33 mg/g for Cu(II), according to the Langmuir isotherm model. The adsorption rates were very fast and reached equilibrium within 3 and 5–10 min for Cu(II) and Pb(II), respectively. In competitive binary metal system, the uptake of Cu(II) largely decreased to 38.40 mg/g, and Pb(II) selectivity was observed. Elemental and functional characterization suggested that the adsorption proceeded by ion exchange between the adsorbent and metal ions. In a flow-through column system, adsorption followed by desorption aided in effectively eluting ~260 mg of Pb(II) (out of ~300 mg total adsorbed) from the Pb(II)–Cu(II) binary solution. Finally, the adsorbent was very effective in four successive adsorption–desorption cycles with over 99 % uptake and 94 % desorption efficiencies. The present study may provide an alternative option for waste fiber recycling and could be useful in recovering heavy metal ions from aqueous sources to complement their depleting reserves.

Keywords Adsorption · Column separation · Eluent · Heavy metal · Reusability · Waste Lyocell fiber

Introduction

Lead and copper are representative examples of a group of metals generally referred as heavy metals. They are among the list of metallic elements that are considered toxic to the environment and humans, especially on long-term exposure. They are classified as priority hazardous substances by various agencies including the Agency for Toxic Substances and Disease Registry (<http://www.atsdr.cdc.gov/SPL/>; Dong et al. 2013; Ge et al. 2014). They are found in the effluents from construction and mining industries, metal processing industries, lead batteries, pigments, printing products, and automobiles (Bailey et al. 1999; Ge et al. 2014; Liu et al. 2008). When the effluents containing these metals are not well handled or treated before their disposal, they pose severe threats to the environment. Moreover, they may cause acute and chronic effects such as encephalopathy (brain dysfunction), nausea, vomiting, anemia, nephropathy (kidney disease), chalcosis of the eye, and metal poisoning (Huang et al. 2013; Nielen and Marvin 2008).

Irrespective of the impacts of heavy metals, their tremendous industrial applications and endless uses cannot be overemphasized. For instance, copper is the third most widely used metal applicable in areas such as construction and electricity owing to its light weight and durability, and in transportation systems for its high ductility. Moreover, its malleability in alloys provides good acoustic properties to be applied in marine systems (<http://www.usesof.net/uses-of-copper.html>). Lead is undoubtedly another important metal of industrial use, only surpassed by iron, copper, zinc, and aluminum. It is used in electrical batteries for vehicles, and its addition in alloys brings about the needed hardness and mechanical resistance to prevent abrasion (<http://nautilus.fis.uc.pt/st2.5/scenes-e/elem/e08230.html>;

✉ Y.-S. Yun
ysyun@jbnu.ac.kr

¹ Division of Semiconductor and Chemical Engineering,
Chonbuk National University, Jeonju, Jeonbuk 561-756,
Republic of Korea



Ngah and Fatinathan 2010). Lead also finds uses in radiation protection, welding, ammunitions, gasoline additives, and manufacturing sheets for roofing (Ngah and Fatinathan 2010). Having realized only a finite amount of metals exist in the earth's crust, the natural reserves containing these metals are estimated to be exhausted in the next few decades because of constant tapping to meet industrial demands but with less efforts to replenish them after use (The National Academy of Sciences 1996). Moreover, most researchers focus on the removal and disposal of these metals rather than their separation and recovery for reuse. However, if they could be separated and retrieved from industrial effluents or other aqueous sources for reuse, they could serve a good course in addressing both environmental safety and resource reclamation problems, and their continuous supply could be maintained to meet industrial demands.

Various techniques have been developed and used to retrieve target compounds from aqueous effluents. Among them is the adsorption technique which is widely used because of its feasibility and application potentials (Saleh and Gupta 2014; Imran and Gupta 2006; Imran 2014; Ding et al. 2012; Pillai et al. 2013). Adsorption as a metal remediation technique is usually credited with simplicity, cost-effectiveness, and eco-friendliness. Compared with other conventional methods, adsorption employs less harmful chemicals and does not produce chunk sludge after operation (Imran and Gupta 2006; Saleh and Gupta 2014; Demirbas 2008; Pillai et al. 2013). The adsorption technique helps to remove metal ions even in minute quantities, which is a challenge to other techniques (Imran and Gupta 2006; Saleh and Gupta 2014; Demirbas 2008; Kaewsarn and Yu 2001). This process also permits selectivity of target metals and regeneration of metal-loaded adsorbents, which is useful for metal separation, recovery, and adsorbent reuse (Liu et al. 2008; Wu et al. 2005). With the volumes of metal-containing effluents that industries need to treat on regular basis, it is always important to find adsorbents that can achieve high-rate removal in continuous flow systems. Several adsorbents have been developed and used to treat wastewater bearing various ionic pollutants (Saleh and Gupta 2014; Imran 2010, 2012a, b; Ding et al. 2012; Pillai et al. 2013). Recently, fibrous adsorbents have received special attention and have been unveiled to have fast metal removal kinetics, a property that permits greater part of their total metal uptake capacities to be realized in flow-through systems (Won et al. 2014).

Furthermore, large amounts of textile fiber wastes are generated annually across the world. For instance in 2012, an estimated amount of 14.3 million tons of textile fiber wastes were generated in the USA alone, and out of this, only 15.7 % was recovered for reprocessing (<http://www.epa.gov/wastes/conservation/materials/textiles.htm>). This

indicates that the remaining percentage of textile fiber wastes will go into waste streams, thus posing environmental issues. Conventional solid waste disposal methods such as landfill and incineration are limited by problems of price escalations, strict environmental regulations, leachate escapes, greenhouse gases, and water and ground pollutions, making textile fiber recycling a cost issue for the textile and fiber processing industries (Cunliffe 1996; Muthu et al. 2012). Meanwhile, these waste textile fibers could be recycled into adsorbent materials with or without eco-friendly chemical modification techniques. The chemical modification could introduce high-affinity binding sites into the fiber matrices, thereby making them applicable to metal adsorption (Chang et al. 2011; Yang et al. 2011).

Considering the aforementioned reasons, waste textile Lyocell fiber was selected as raw material to prepare chemically modified adsorbent via carboxymethylation process. Lyocell is manufactured from the naturally abundant wood cellulose. The Lyocell fiber is relatively thin and can be obtained very cheaply from textile/fiber processing residues; however, it contains no active functional groups for binding heavy metal ions. Carboxymethylation is an effective method for preparing adsorbents with high-affinity carboxyl groups, which are used in various applications including adsorption of heavy metal ions (Pushpamalar et al. 2006; Bediako et al. 2015a). By this process, the waste Lyocell fiber adsorbent was successfully prepared and applied to adsorption and separation of Pb(II) and Cu(II) from their aqueous mixtures. To gain pre-knowledge into the adsorption equilibrium behavior and binding mechanisms of the metal ions, batch adsorptions were first studied. Regeneration and reuse of the adsorbent were also investigated to assess its potential use over several adsorption cycles.

The study described in this paper was wholly carried out at the Division of Semiconductor and Chemical Engineering, Chonbuk National University (South Korea), between September 2014 and June 2015.

Materials and methods

Materials

The materials used in this study are listed as follows: Isopropyl alcohol (99.5 %), sodium chloroacetate (SCA, 98 %), and epichlorohydrin (ECH, 99 %) were purchased from Sigma-Aldrich Co., Korea; NaOH from Daejung Chemical & Metals Co. Ltd; methanol from SK Chemicals, Ulsan Korea; ethyl alcohol (94 %) from Duksan Pure Chemical Co.; and nitrate complexes of copper and lead from Junsei Chemical Co. Pre-consumer waste Lyocell



strands of approximately 12 μm were received from a fiber processing company in Korea. Double-distilled water (DW) was used throughout the study in preparing solutions and washing samples when required.

Methods

Adsorbent preparation by carboxymethylation reaction

Carboxymethylation reaction (CMR) was carried out according to Williamson's ether synthesis (Pushpamalar et al. 2006; Tijssen et al. 2001). In brief, aqueous NaOH (30 % w/v, 10 mL) was added to a solution of isopropyl alcohol and water (80:20 v/v), followed by addition of 3 g of Lyocell fiber strands. The solution containing fiber strands was placed in a multi-shaking incubator maintained at 45 °C/160 rpm, and 10 g of SCA was added to start the CMR. The reaction was allowed for 5 h after which the fibers were taken and re-suspended in methanol to terminate the reaction. At this point, the fibers could not be washed in water as they were highly hydrophilic and susceptible to dissolution.

Crosslinking of the carboxymethylated adsorbent

To provide water stability, the resulted carboxymethylated adsorbent was crosslinked to prevent solubility because of its high hydrophilicity after the CMR. To do that, solid NaOH (5 g) was dissolved in 100 mL of ethyl alcohol measured into a 200-mL glass bottle, followed by addition of 20 mL ECH. The carboxymethylated fibers were then added, and the entire content was placed in a shaker at 45 °C for 24 h. The crosslinked adsorbent was washed thoroughly with methanol, rinsed with distilled water to neutral pH, and

freeze-dried to a constant weight. Scheme 1 shows the chemical reactions for carboxymethylation and crosslinking. To confirm that crosslinking was effectively achieved, both crosslinked and non-crosslinked fibers were placed in DW. After few hours (~ 6 h), the non-crosslinked fibers dissolved, while the crosslinked fibers were still intact.

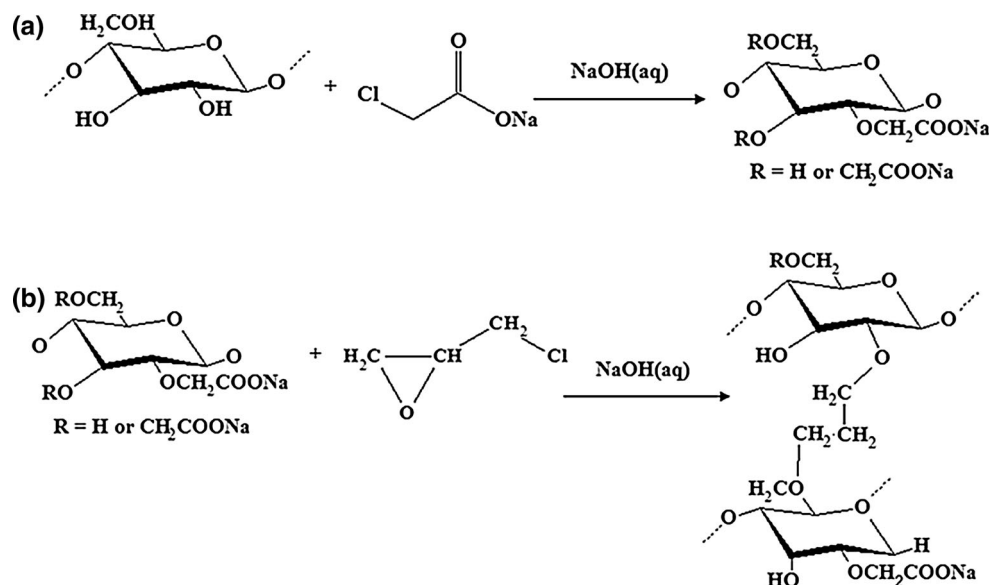
Batch adsorption experiments

Stock solutions of Pb(II) and Cu(II) were prepared from $\text{Pb}(\text{NO}_3)_2$ and $\text{Cu}(\text{NO}_3)_2 \cdot 3\text{H}_2\text{O}$, respectively, and were diluted further into working solutions of different concentrations. Thirty milliliters (30 mL) each of the working solutions containing metal nitrates of Pb(II) and Cu(II) of known concentrations in the range of 10–1000 mg/L was added to weighed amounts of the prepared adsorbent (~ 0.03 g) for batch adsorption studies. The pHs of the solutions were adjusted with 1 M HNO_3 or NaOH whenever deviations were noticed. Adsorbent reusability study was performed by batch adsorption and desorption tests to evaluate the reuse potential of the adsorbent. For this, 200 mg/L of Pb(II) solution was used, and four cycles of adsorption and desorption were run. After each adsorption, the metal-loaded adsorbent was washed with DW before desorbing in 1 M HCl solution. The residual DW together with the acid solution containing desorbed metal ions was analyzed for Pb(II) concentration.

Column adsorption and metal separation

Column setup was run, and samples were taken at predetermined times from the column outlet for analyses. A borosilicate glass column (Omnifit Ltd., USA) of 1.0 cm diameter and 10.0 cm length was packed with 5 mL of the

Scheme 1 Chemical modification reactions; **a** carboxymethylation, **b** crosslinking



adsorbent weighing 0.46 g, and a mixed solution of Pb(II) and Cu(II) (~ 200 mg/L) was pumped from the bottom upward through the column using a peristaltic pump. Other experimental conditions used are as follows: initial pH = 5.10; final pH = 4.74; and flow rate = 1.4 mL/min. A 1 M HCl solution was used for desorption and was run through the column at the same flow conditions as in the adsorption process. The residual metals after the adsorption and desorption experiments were analyzed using an inductively coupled plasma spectrometer (Shimadzu, ICP-7510, Japan) after centrifugation, and samples were diluted when necessary. The metal uptakes after the ICP analysis were calculated by Eq. 1.

$$q_e = \frac{(C_i - C_e)V}{M} \quad (1)$$

where q_e is the equilibrium Cu(II) or Pb(II) uptake, C_i and C_e are, respectively, the initial and equilibrium concentrations in mg/L, V is the volume in L, and M is the dry mass of sorbent in g.

Adsorbent characterization (before and after adsorption)

The metal-loaded and unloaded adsorbents were freeze-dried and characterized using an SEM/EDX system and FTIR spectrometer. The surface morphologies and elemental peaks of the unloaded and loaded adsorbents were analyzed using a combined WDS/EDS scanning electron microscope, SEM (JEOL, JSM-6000 series WDS/EDS system, Japan). The surfaces of the samples were coated with Au before the

analysis. FTIR analysis was performed using a PerkinElmer spectrometer (FTIR/NIR spectrometer) to confirm attachments between the metals and the adsorbent's active sites after adsorption. The FTIR spectra were measured in the wavelength band range of $4000\text{--}400\text{ cm}^{-1}$.

Isotherm and kinetic models applied

To investigate the isotherm and kinetics of Pb(II) and Cu(II) adsorption in this study, three widely used isotherm models, namely Langmuir (1918), Freundlich (1906), and Redlich–Peterson (1959) models, and two kinetic models, pseudo-first- and pseudo-second-order models (Ho and McKay 1999; Lagergren 1898), were used to fit and describe the data obtained. The Langmuir model describes monolayer adsorption onto an adsorbent at specific homogeneous sites; the Freundlich model applies to both monolayer and multilayer adsorption onto an adsorbent's heterogeneous surface; and the Redlich–Peterson model is the incorporation of both the Langmuir and Freundlich models with constant values of near unity and 0 depicting Langmuir and Freundlich isotherms, respectively (Mao et al. 2011; Pillai et al. 2013). The pseudo-first-order model describes the adsorption in solid–liquid systems based on the adsorption capacity of solids by assuming one adsorbate to one adsorption site phenomenon (Boparai et al. 2011; Lagergren 1898). The pseudo-second-order model describes the chemisorption kinetics from liquid solutions (Azizian 2004; Ho 2006; Lagergren 1898). The model equations are expressed in their nonlinear forms in Table 1.

Table 1 Adsorption isotherm and kinetic models and their interpretations

Models	Parameters	Interpretations
<i>Langmuir model</i>	q_{\max} (mg/g)	Maximum adsorbate uptake
$q = q_{\max} \frac{bC_f}{1+bC_f}$	b (L/mg)	Affinity between adsorbent and adsorbate
	q (mg/g)	Equilibrium adsorbate amount
	C_f (mg/L)	Adsorbate concentration at equilibrium
<i>Freundlich model</i>	q_e (mg/g)	Equilibrium adsorbate uptake
$q_e = kC_e^{1/n}$	k (L/g)	Freundlich constant
	C_e (mg/L)	Equilibrium adsorbate concentration
	n	Constant denoting intensity of adsorption
<i>Redlich–Peterson model</i>	q (mg/g)	Maximum adsorbate uptake
$q = K_{RP} \frac{C_f}{1+a_{RP}C_f^{\beta_{RP}}}$	C_f (mg/L)	Adsorbate concentration at equilibrium
	K_{RP} (L/mg)	Redlich–Peterson isotherm constant
	a_{RP} (L/mg)	Redlich–Peterson isotherm constant
	β_{RP}	Redlich–Peterson model exponent
<i>Pseudo-first-order model</i>	q_1 (mg/g)	Equilibrium adsorbate amount
$q_t = q_1(1 - \exp(-k_1t))$	q_t (min)	Amount of adsorbate adsorbed at any time
	k_1 (L/min)	First-order equilibrium rate constant
<i>Pseudo-second-order model</i>	q_2 (mg/g)	Equilibrium adsorbate amount
$q_t = \frac{q_2^2 k_2 t}{1+q_2 k_2 t}$	q_t (min)	Amount of adsorbate adsorbed at any time
	k_2 (g/mg min)	Second-order equilibrium rate constant



Results and discussion

Isotherm of single and binary metal solution systems

Adsorption isotherm represents the amount of materials adsorbed onto the surface of an adsorbent as a function of the materials present in solution at a constant temperature. It is used to estimate the maximum adsorption capacity of an adsorbent, and the affinity between the adsorbent and adsorbate, which determines whether the adsorption process is favorable or not (Basha et al. 2008; Febrianto et al. 2009; Ho et al. 2002; Mao et al. 2011). The adsorption isotherm experiments in this study were conducted in single solutions of Cu(II) and Pb(II) at the respective pH values of 4 and 5 and in binary metal solutions at pH 4. These pH conditions were found suitable for effective adsorption of the two metals without precipitations, based on previous studies (Bediako et al. 2015b; Ge et al. 2014; Li et al. 2015; Liu et al. 2008). From the present data, the maximum uptakes, affinities, and intensities of adsorption were estimated by fitting the data to the Langmuir, Freundlich, and Redlich–Peterson isotherm models (Table 1). In the single metal solutions, the Langmuir isotherm model well fitted the experimental data. The three-parameter Redlich–Peterson model provided fittings similar to the two-parameter Langmuir model. The value of the Redlich–Peterson model exponent, β_{RP} , was close enough to 1, depicting a Langmuir adsorption isotherm. The Langmuir model's b value that relates the affinity between the adsorbate and adsorbent predicted a stronger affinity toward Cu(II). The Freundlich model could not adequately represent the isotherm data in this study; however, its higher n value for Cu(II) also strengthened the assertion that the binding affinity for Cu(II) was stronger and more intensive.

A higher Pb(II) uptake (353.45 mg/g) was obtained, and the underlying reasons could be attributed to factors such as functional group charges, distribution coefficients (i.e., metal mobility in solution), and periodic properties (e.g., electronegativity) (Li et al. 2011; Liu et al. 2008; Sheng et al. 2007; Kaewsarn and Yu 2001). Generally, higher electronegativity and easier mobility of metal ions in solution mean higher reactivity (Li et al. 2011; Liu et al. 2008; Sheng et al. 2007). The electronegativity and distribution coefficients of Pb(II) are greater, hence justifying its higher uptake. The fact that deprotonation of carboxyl binding sites increases with increasing pH also influenced the higher uptake of Pb(II) since it was done at a higher pH than Cu(II). For both metals, however, the uptakes increased initially and reached saturation at higher concentrations (Fig. 1a). Similar adsorption trends were observed in several other studies involving heavy metal

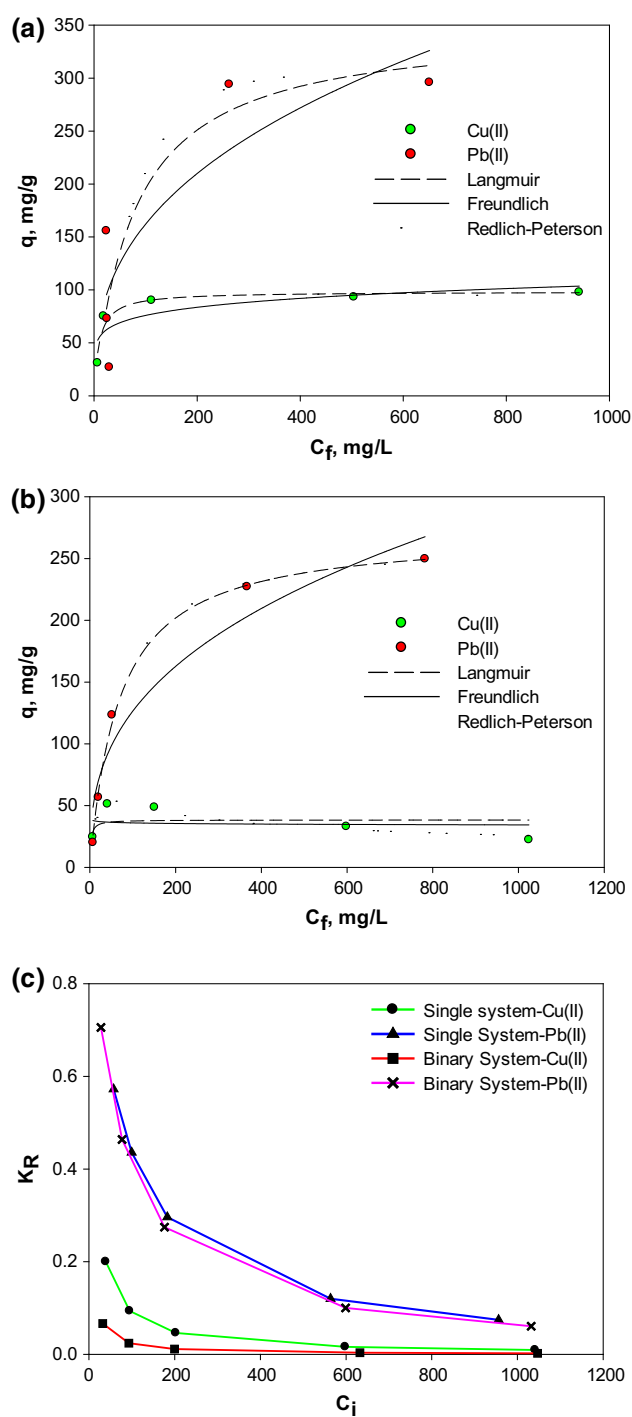


Fig. 1 Single and binary metal isotherms of Pb(II) and Cu(II) adsorptions; **a** single metal system, **b** binary metal system, **c** plot of K_R against initial concentration of Pb(II) and Cu(II)

ions (Saleh and Gupta 2012a; Saleh 2015; Saleh et al. 2011; Dong et al. 2013; Gupta et al. 2013; Liu et al. 2008). This suggests that at the initial lower concentrations there were sufficient binding sites to accommodate greater portions of the metal ions, but these sites got saturated with



increase in metal concentrations so that no more metal ions could be attached at the higher concentrations.

Adsorption studies in the binary metal systems were conducted at pH 4 in order to prevent precipitation, specifically copper (Bediako et al. 2015b). Adsorption at lower concentrations appeared very competitive compared with those at higher concentrations where Pb(II) selectivity was observed. In other words, both Pb(II) and Cu(II) were almost equally adsorbed when their concentrations were lower (i.e., ≤ 100 mg/L), but as their concentrations increased, the competition for the occupancy of the limited binding sites became more intense and hence Pb(II) was preferentially adsorbed. This consequently led to an unusual isotherm shape for the Cu(II) adsorption in the Pb(II)–Cu(II) binary system. Thus, a sharp increase in the uptake of Cu(II) occurred at the beginning of sorption; however, a sudden fall was observed midway toward equilibrium (Fig. 1b).

The effect of the isotherm shape can be used to predict the favorability of an adsorption process (Ho et al. 2002). From the essential features of the Langmuir isotherm which best describes the present data, a dimensionless constant known as the separation factor or equilibrium parameter K_R can be expressed by Eq. 2 (Hall et al. 1966; Ho et al. 2002).

$$K_R = \frac{1}{1 + bC_i} \quad (2)$$

where K_R is the dimensionless separation factor; C_i is the initial concentration (mg/L); and b is the Langmuir constant (L/mg). For $K_R > 1$, the adsorption is deemed unfavorable; for $K_R = 1$, the adsorption is linear; for $0 < K_R < 1$, the adsorption is considered favorable; and $K_R = 0$ indicates that the adsorption is irreversible (Hall et al. 1966; Ho et al. 2002). The K_R values for Pb(II) and Cu(II) adsorptions in both the single and binary solutions were calculated and plotted as shown in Fig. 1c. The K_R values indicated that the adsorption of both metals was more favorable at higher initial concentrations in both the single and binary systems; however, Cu(II) adsorption was more favorable than Pb(II) adsorption. With Cu(II) adsorption being more favorable, the reason for the preferential adsorption of Pb(II) in the binary system could

therefore be explained by the displacement and repulsion mechanisms. Although Cu(II) adsorption was supposedly favored, Pb(II) exhibited greater inhibitory effects, especially at higher concentrations, such that it was able to push significant portion of the initially adsorbed Cu(II) back into the solution when the adsorption became very competitive. This phenomenon is consistent with that observed by Sheng et al. (2007) in the biosorption of Pb(II), Cu(II), and Cd(II) onto a marine algae, but is not in agreement with the adsorption of same metals using cellulose waste xanthate (CWX) (Bediako et al. 2015b), iminodiacetic acid (IDA)-chelating resin (Li et al. 2011), and diethylenetriamine (DETA)-functionalized adsorbent (Liu et al. 2008). In the previous study using cellulose waste xanthate (Bediako et al. 2015b) and in the studies by Li et al. (2011) and Liu et al. (2008) using IDA- and DETA-related adsorbents, respectively, Cu(II) selectivity was observed. Notably, IDA, DETA, and xanthate all contain metal-chelating groups which form more stable complexes with Cu(II) than with Pb(II). As described in the sections ahead, ion exchange was the dominant mechanism of adsorption in this study. Unlike chelation, ion exchange does not form metal complexes, and so adsorbent–metal complex stability could not play a major role in the selective adsorption observed in this study. Extract from this phenomenon would indicate that the selectivity of metal ions adsorption largely depends on the functional groups present on/in the adsorbent, the metal-binding mechanisms (i.e., chelation or ion exchange), and the characteristics of the metal ions in solution.

The inhibitory effect of Pb(II) on Cu(II) could also be explained on the basis of other periodic properties of lead and copper. The valence electrons of lead exist comparatively far from the nucleus and are thus at higher principal quantum numbers and higher potential energies than those of copper (IUPAC 1997; Murrell et al. 1985; Partington 1921). These properties depict high antagonism and high reactivity. Hence in the binary solution, Pb(II) could easily displace Cu(II) which could not compete with the strong antagonism induced by Pb(II), especially at higher concentrations. Owing to the uneven nature of the isotherm curve of Cu(II) in the binary solution, the two-parameter Langmuir and Freundlich models could not properly fit its

Table 2 Langmuir, Freundlich, and Redlich–Peterson model parameters of single and binary metal isotherms of Cu(II) and Pb(II) adsorption

Solution type	Metals	Langmuir model			Freundlich model			Redlich–Peterson model			
		q_{\max} (mg/g)	b (L/mg)	R^2	k (L/g) $^{1/n}$	n	R^2	K_{RP} (L/mg)	a_{RP} (L/mg)	β_{RP}	R^2
Single metal	Pb(II)	353.45	0.013	0.914	29.867	2.701	0.747	3.516	0.002	1.241	0.928
	Cu(II)	98.33	0.102	0.926	40.144	7.226	0.702	8.506	0.067	1.042	0.936
Binary metal	Pb(II)	321.33	0.015	0.998	23.564	2.741	0.949	3.766	0.011	1.031	0.998
	Cu(II)	38.40	0.438	0.112	39.404	−51.38	0.014	3.924	0.014	1.347	0.963



Table 3 Parameters of the pseudo-first- and pseudo-second-order models for single and binary metal kinetics

Solution type	Metal	Pseudo-first-order			Pseudo-second-order		
		q_1 (mg/g)	k_1 (L/min)	R^2	q_2 (mg/g)	k_2 (g/mg min)	R^2
Single metal	Pb(II)	307.32	1.188	0.991	233.21	0.010	0.998
	Cu(II)	84.80	1.767	0.999	85.85	0.060	0.997
Binary metal	Pb(II)	294.89	0.794	0.961	212.95	0.006	0.993
	Cu(II)	31.92	2.174	0.941	42.34	0.175	0.942

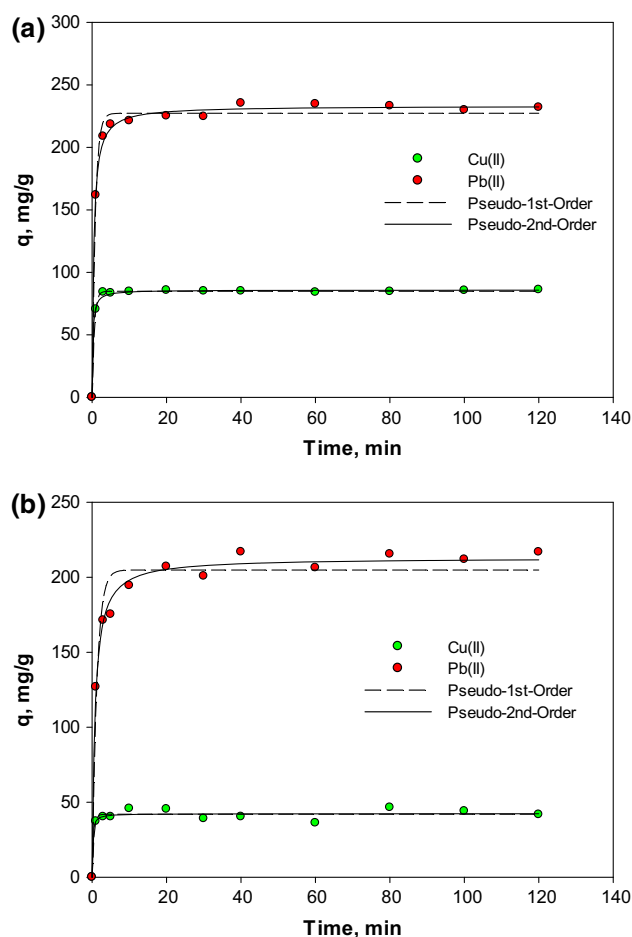
data. As presented in Table 2, the R^2 values were very low. In contrast, all the data fitted well to the three-parameter Redlich–Peterson model with high R^2 values.

Kinetics of single and binary metal adsorption

Kinetics represents the removal rate of adsorbates from the solution phase as a function of time. It estimates the time lapse between the initial adsorption and saturation (Azizian 2004). The kinetic studies of single and binary metals were performed for 120 min within which samples were taken at predefined intervals and analyzed. The data obtained indicated that the metal adsorption rates in both systems were much faster, reaching equilibria in just ~ 3 min and 5–10 min for Cu(II) and Pb(II), respectively. The relatively thin fiber sizes might have enabled the fast adsorption rates as the metal ions could easily access the binding sites which reside mostly on the surface of the adsorbent. The initial steep slopes confirmed the extremely fast binding rates, and this is particularly very essential in practical adsorption applications, where large amounts of effluents need to be treated within shorter time paces (Azizian 2004; Sheng et al. 2007). The slightly faster binding kinetics of Cu(II) than Pb(II) confirmed the earlier observation in the isotherm studies, portraying high affinity of the adsorbent toward Cu(II). However, the stronger inhibitory force offered by Pb(II) toward Cu(II) in the binary solution led to the drastic uptake decrease of the latter. The kinetics data were described by the pseudo-first- and pseudo-second-order kinetic models and are summarized in Table 3 and Fig. 2. The rate models closely predicted the equilibrium uptakes in both systems, however, with slightly higher precisions (higher R^2 values) in the single systems than in the binary systems. This observation was not unexpected because of the high competition among metal ions in the binary systems which adversely affected their adsorption trends and efficiencies.

Column adsorption and metal separation

To separate Pb(II) and Cu(II), a column adsorption followed by desorption was carried out. This process helped in effectively obtaining only Pb(II) solution after Cu(II) was fully desorbed within the first 5 min of desorption. In

**Fig. 2** Kinetics of **a** single metal and **b** binary metal adsorptions of Pb(II) and Cu(II)

the column setup, 5 mL of solution was retained for every 3.57 min and discharged at the rate of 1.4 mL/min. During the adsorption, the Cu(II) uptake was very rapid, reaching breakthrough and exhaustion in shorter time just as it was observed in the batch adsorption studies (Fig. 3a, b). The breakthrough and exhaustion times of Pb(II) were quite extended and showed higher cumulative uptakes (Fig. 4a, b). The breakthrough and exhaustion times were deduced from the plot of C_{out}/C_{in} verses time or bed number and were estimated as the time when the output metal concentration reached 10 % and exceeded 95 % of the input concentration, respectively. The cumulative uptakes were



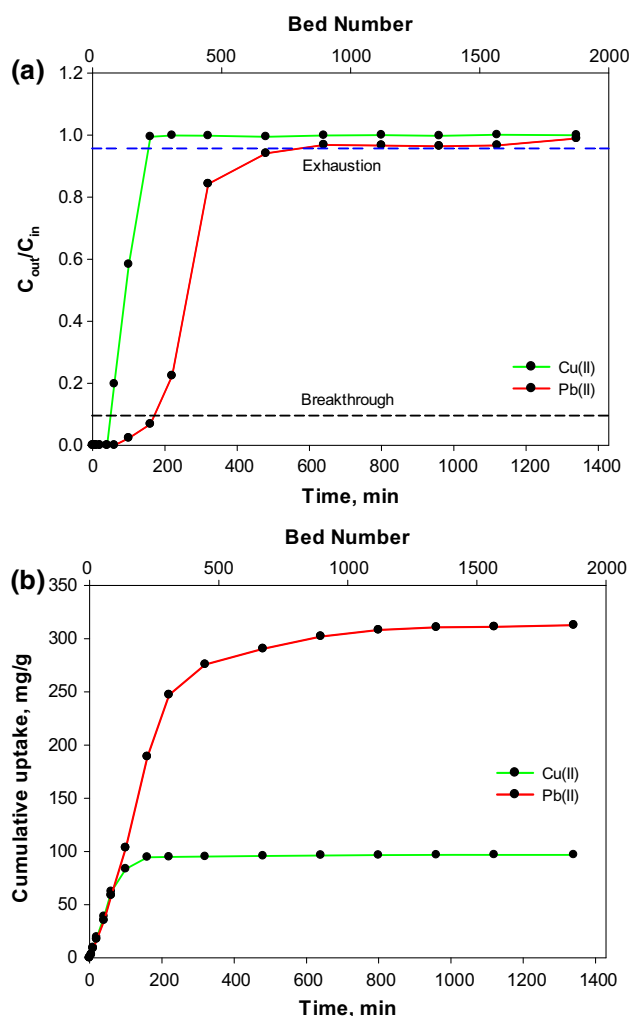


Fig. 3 Column results of Pb(II)-Cu(II) binary sorption: **a** breakthrough curves, **b** cumulative uptake curves: Cu(II) breakthrough time = 48 min; Pb(II) breakthrough time = 175 min; Cu(II) exhaustion time = 156 min; Pb(II) exhaustion time = 598 min

estimated by integrating the changes in the metal concentrations over the adsorption time at constant flow rate and adsorbent weight. The integration is mathematically expressed by Eq. 3.

$$q_t = \frac{Q}{M} \int_0^t [C_{in} - C_{out}] dt \quad (3)$$

where q_t (mg/g) is the metal uptake at time, t (min), C_{in} (mg/L) is the input metal concentration, C_{out} (mg/L) is the output metal concentration at any given time, Q (mL/min) is the flow rate of the solution through the column, and M (g) is the dry mass of the adsorbent. Consequently, the cumulative uptakes of Pb(II) and Cu(II) were 312.66 and 98.84 mg/g, respectively. The separation of the metal ions was unachievable by adsorption; however, in the follow-up desorption step using 1 M HCl as the eluent, the separation

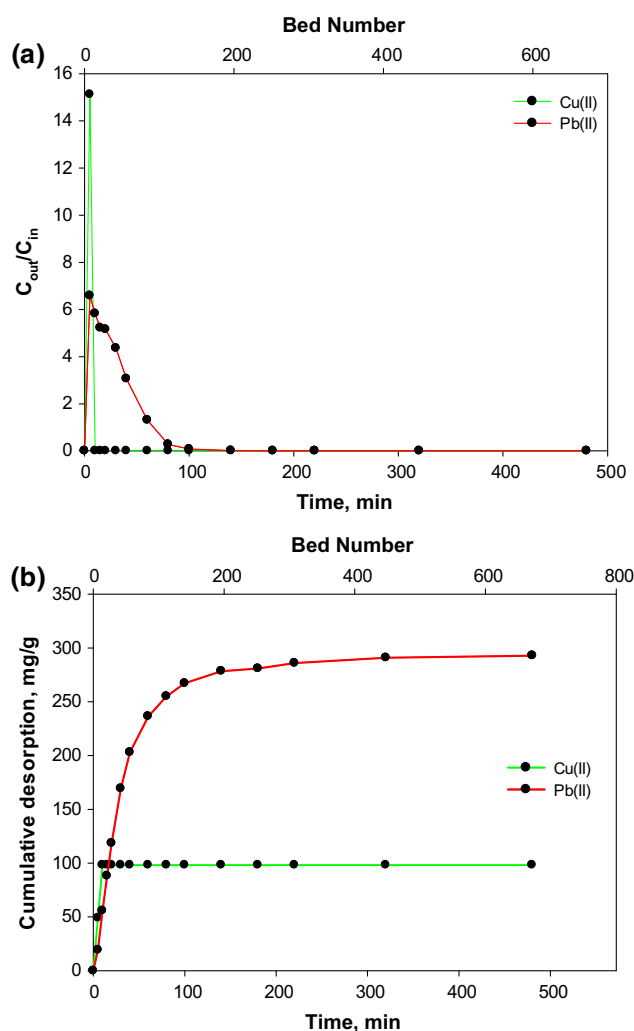


Fig. 4 Column separation of Pb(II) from Pb(II)-Cu(II) binary mixture **a** desorption breakthrough curves, **b** cumulative desorption curves

was achieved. Within the first 5 min, all of Cu(II) (~ 100 mg) was desorbed along with a negligible amount of Pb(II), and soon after, only Pb(II) was detected at the column outlet until 180 min when equilibrium was reached. This was made possible as a result of the fast desorption rate of Cu(II), leaving behind only Pb(II). Consequently, ~ 260 mg of Pb(II) was obtained at the end of the desorption process.

Regeneration and reusability evaluation of adsorbent

Adsorbents should be essentially regenerated without significant loss in efficiency in order to be applicable on practical scales. Thus, the reusability of the adsorbent was performed to test its efficiency. Figure 5 shows the efficiency of each of the four adsorption-desorption cycles in percentages, indicating that the adsorbent exhibited over



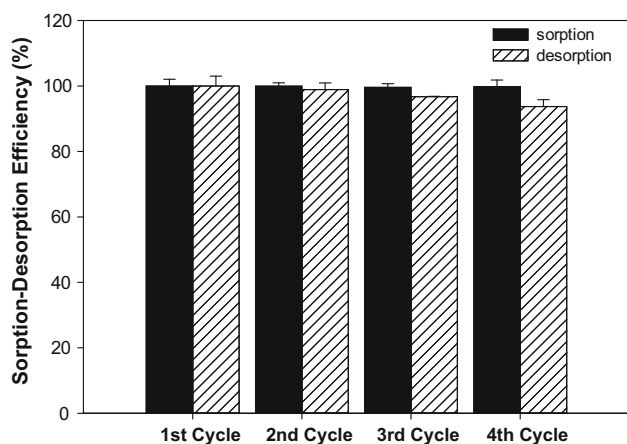


Fig. 5 Sorption and desorption efficiency (%) of sorbent using Pb(II) solution

99 % adsorption efficiency even at the fourth cycle, out of which ~94 % was desorbed. There were no traces of Pb(II) in the DW used in washing the metal-loaded adsorbent prior to desorption. This together with the negligible decrease in adsorption efficiency over the four

cycles indicates that there was no leaching, and the adsorbent can be reused severally.

Elemental analysis, surface morphology, and mechanism of adsorption

Figure 6 shows the results of SEM and EDX of the metal-loaded and unloaded adsorbents. The unloaded adsorbent showed well-arranged fibers with very smooth surfaces; however, the metal-loaded fibers appeared shrunk with wrinkled surfaces. The size (thickness) of the fiber strands increased from ~12 to ~16 μm after the chemical modifications. From the EDX graphs, it could be observed that the Na peak in the unloaded sample disappeared after adsorption, while Pb and Cu peaks emerged in the metal-loaded sample. This indicates that Na(I) was fully displaced in exchange for Pb(II) and Cu(II) during the adsorption, which also indicates adsorption by ion exchange (Scheme 2). Upon displacement of Na(I) ions, the carboxyl groups on the adsorbent become negatively charged and thus ready to attract the positively charged Pb(II) or Cu(II) ions (Scheme 2a). This mechanism also indicated that each

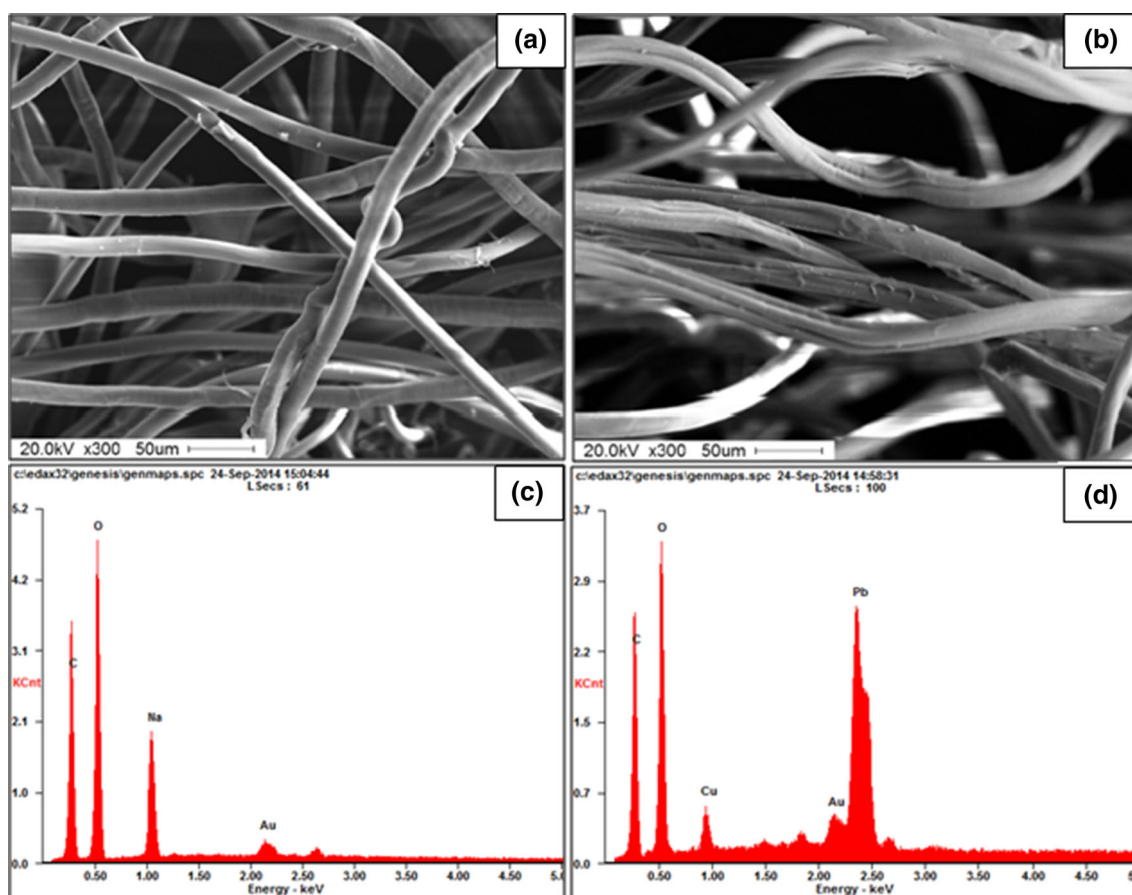
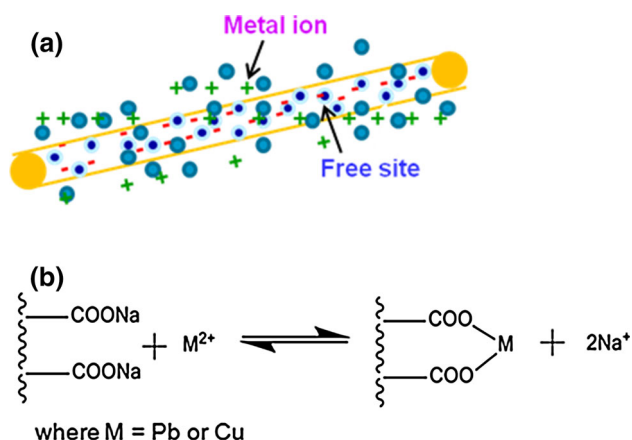


Fig. 6 SEM and EDX analyses: **a** morphology of unloaded sorbent, **b** morphology of loaded sorbent, **c** elemental peaks of unloaded sorbent, and **d** elemental peaks of loaded sorbent



Scheme 2 Ion exchange mechanism of Pb(II) and Cu(II) adsorption; **a** diagrammatic representation, **b** schematic representation

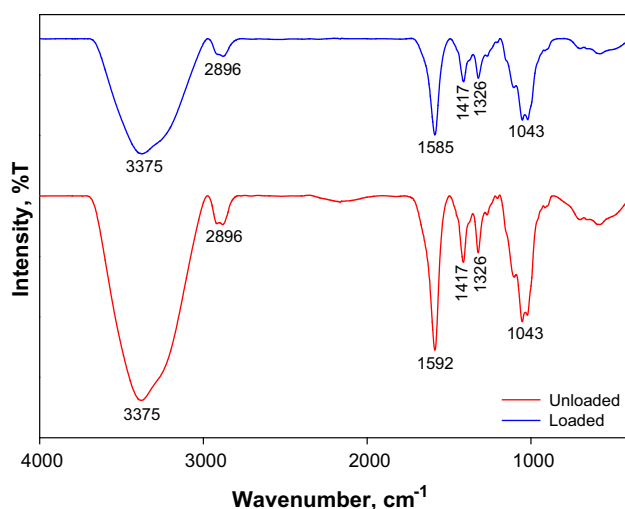


Fig. 7 FTIR analysis of the metal-loaded and unloaded sorbents

metal species was trapped between the two carboxyl binding sites on the adsorbent as shown in Scheme 2b. Ion exchange has been identified as the dominant metal-binding

mechanism in most studies involving carboxyl groups (Mitic-Stojanovic et al. 2011; Sheng et al. 2007).

Apart from the ion exchange observed in the EDX spectra, the adsorption process was also studied by the FTIR spectra of the adsorbent before and after metal adsorption (Fig. 7). FTIR spectra are widely employed in analyzing the presence of functional groups in/on adsorbent materials (Saleh and Gupta 2014). In some cases, they are used to identify which groups are involved in the binding of target ions through peak alterations (Gupta et al. 2011). Therefore, FTIR has been used in this study to identify the functional groups present on the prepared adsorbent and the groups involved in the metal-binding process. Before adsorption, the unloaded adsorbent showed very intense characteristic peaks such as strong OH (3375 cm^{-1}), C-H (2896 cm^{-1}), COO^- (1592 cm^{-1}), CH_2 (1417 cm^{-1}), C-O (1326 cm^{-1}), and CH-O-CH_2 (1043 cm^{-1}) (El-Zawawy 2006; Hebeish et al. 2013; Pushpamalar et al. 2006; Bediako et al. 2015a; Yang et al. 2011; Saleh and Gupta 2012b). After the adsorption, major peak shifts particularly the peak at 1592 cm^{-1} , representing carboxyl groups, was observed (Saleh 2011; Saleh and Gupta 2011; Bediako et al. 2015a). These peak shifts indicated the formation of coordinate bonds between the carboxyl binding sites and the metal ions. Therefore, the FTIR analysis also confirmed the assertion that Pb(II) and Cu(II) interacted through the negatively charged carboxyl groups of the adsorbent.

Comparison of adsorption performance

Several works have been reported on the application of different adsorbents to treat toxic pollutants in wastewater effluents (Saleh and Gupta 2014; Imran 2010, 2012a, b; Ding et al. 2012; Pillai et al. 2013). Some of the adsorbents showed promising prospects for large scale and commercial applications, while others may only serve research needs. It is thus important to compare the performance of newly developed adsorbents with existing ones so as to assess their

Table 4 Comparison of the prepared adsorbent with recently reported adsorbents

Adsorbent	Uptake, q_{max} (mg/g)		pH	Kinetics	References
	Pb(II)	Cu(II)			
Activated date stone	154	–	6.5	10 min	Abudaia et al. (2013)
Aminated lignin	66.5	89.4	5/6	–	Ge et al. (2014)
Lignin-based dithiocarbamate	103.5	176	5/6	30/20 min	Ge et al. (2014)
Sulfonated cotton linters	37.5	–	6	8 min	Dong et al. (2013)
Cellulose waste xanthate	–	123.4	4	5 min	Bediako et al. (2015a, b)
IDA-chelating resin	263.1	–	5	6 h	Li et al. (2011)
Lignin xanthate	63.9	–	5	90 min	Li et al. (2015)
DETA-functionalized	–	76.3	5	100 min	Liu et al. (2008)
Carboxymethylated Lyocell	353.5	98.3	5/4	5/3 min	This study



competitiveness. In this regard, the performance of the prepared carboxymethylated Lyocell adsorbent was compared with some reported ones (Table 4). In the studies of Dong et al. (2013) using sulfonated cotton linters, only a maximum of 37.45 mg/g Pb(II) uptake was recorded even though the adsorption experiment was performed at a high pH value (pH 6). Furthermore, the performance of porous lignin xanthate resin showed relatively low performance in terms of Pb(II) uptake capacity and kinetics (Li et al. 2015). In the studies by Abudaia and co-workers where activated carbon was prepared from date stone, the affinity of the prepared adsorbent toward Cu(II) and Pb(II) was so low such that high adsorbent dose of 1 g/100 mL of the metal solutions was required (Abudaia et al. 2013). The uptakes were, however, very low although the studies were conducted at a higher pH of 6.5. Information on the stability of the above-reported adsorbents was not provided; however, the current adsorbent prepared by carboxymethylation and crosslinking is very stable and showed better performance in terms of uptake capacity, kinetics, and reusability.

Conclusion

This study was aimed to study the batch heavy metal adsorption properties of the adsorbent prepared via carboxymethylation and crosslinking of waste Lyocell fiber, and the separation of the metals in column. The batch adsorption studies indicated stronger affinity toward Cu(II) in both single and binary solutions; however, Pb(II) was selectively adsorbed in the Pb(II)–Cu(II) binary solution via displacement and repulsion mechanisms. Other underlying reasons were attributed to factors such as functional group charges, distribution coefficients, and periodic properties of the elements. Step-wise column operation was used to effectively elute and separate Pb(II) from the Pb(II)–Cu(II) binary mixture. Four consecutive adsorption–desorption cycles were found sufficient to prove that the adsorbent has a potential to be regenerated and reused. This study may provide waste fiber recycling alternative and help recover heavy metal ions from aqueous solutions in order to complement their depleting reserves and reduce their negative effects on the environment.

Acknowledgments This work was supported by the Korean Government through NRF (2014R1A2A1A09007378) Grants.

References

- Abudaia JA, Sulyman MO, Elazaby KY, Ben-Ali SM (2013) Adsorption of Pb (II) and Cu (II) from aqueous solution onto activated carbon prepared from dates stones. *Int J Environ Sci Dev*. doi:10.7763/ijesd.2013.v4.333
- Azizian S (2004) Kinetic models of sorption: a theoretical analysis. *J Colloid Interface Sci* 1:47–52
- Bailey SE, Olin TJ, Bricka RM, Adrian DD (1999) A review of potentially low-cost sorbents for heavy metals. *Water Res* 11:2469–2479
- Basha S, Murthy ZVP, Jha B (2008) Sorption of Hg(II) from aqueous solutions onto Carica papaya: application of isotherms. *Ind Eng Chem Res* 3:980–986
- Bediako JK, Wei W, Yun Y-S (2015a) Sorptive removal of cadmium ions from solution phases using textile fiber waste coated with carboxymethyl cellulose. *Adv Mater Res* 1130:631–634
- Bediako JK, Wei W, Kim S, Yun Y-S (2015b) Removal of heavy metals from aqueous phases using chemically modified waste Lyocell fiber. *J Hazard Mater*. doi:10.1016/j.jhazmat.2015.07.033
- Boparai HK, Joseph M, O'Carroll DM (2011) Kinetics and thermodynamics of cadmium ion removal by adsorption onto nano zerovalent iron particles. *J Hazard Mater* 1:458–465
- Chang CY, He M, Zhou JP, Zhang LN (2011) Swelling behaviors of pH- and salt-responsive cellulose-based hydrogels. *Macromolecules* 6:1642–1648
- Cunliffe J (1996) Recycling textile and plastic waste. Woodhead Publishing Limited, Cambridge
- Demirbas A (2008) Heavy metal adsorption onto agro-based waste materials: a review. *J Hazard Mater* 2–3:220–229
- Ding Y, Jing DB, Gong HL, Zhou LB, Yang XS (2012) Biosorption of aquatic cadmium(II) by unmodified rice straw. *Bioresour Technol*. doi:10.1016/j.biortech.2012.01.110
- Dong C, Zhang H, Pang Z, Liu Y, Zhang F (2013) Sulfonated modification of cotton linter and its application as adsorbent for high-efficiency removal of lead(II) in effluent. *Bioresour Technol*. doi:10.1016/j.biortech.2013.07.108
- El-Zawawy WK (2006) Blended graft copolymer of carboxymethyl cellulose and poly(vinyl alcohol) with banana fiber. *J Appl Polym Sci* 3:1842–1848
- Febrianto J, Kosasih AN, Sunarso J, Ju Y-H, Indraswati N, Ismadji S (2009) Equilibrium and kinetic studies in adsorption of heavy metals using biosorbent: a summary of recent studies. *J Hazard Mater* 2–3:616–645
- Freundlich HMF (1906) Über die adsorption in Lösungen. *Z Phys Chem* 57:385–470
- Ge Y, Xiao D, Li Z, Cui X (2014) Dithiocarbamate functionalized lignin for efficient removal of metallic ions and the usage of the metal-loaded bio-sorbents as potential free radical scavengers. *J Mater Chem A* 7:2136–2145
- Gupta VK, Agarwal S, Saleh TA (2011) Chromium removal by combining the magnetic properties of iron oxide with adsorption properties of carbon nanotubes. *Water Res* 45:2207–2212
- Gupta VK, Agarwal S, Singh P, Pathania D (2013) Acrylic acid grafted cellulosic Luffa cylindrical fiber for the removal of dye and metal ions. *Carbohydr Polym* 98:1214–1221
- Hall KR, Eagleton LC, Acrivos A, Vermeulen T (1966) Pore- and solid-diffusion kinetics in fixed-bed adsorption under constant-pattern conditions. *Ind Eng Chem Fund* 2:212–223
- Hebeish A, Hashem M, Abd El-Hady MM, Sharaf S (2013) Development of CMC hydrogels loaded with silver nanoparticles for medical applications. *Carbohydr Polym* 1:407–413
- Ho Y-S (2006) Review of second-order models for adsorption systems. *J Hazard Mater* 3:681–689
- Ho YS, McKay G (1999) Pseudo-second order model for sorption processes. *Process Biochem* 34:451–465
- Ho YS, Huang CT, Huang HW (2002) Equilibrium sorption isotherm for metal ions on tree fern. *Process Biochem* 37:1421–1430
- <http://www.atsdr.cdc.gov/SPL/>, ATSDR. Retrieved 2015.04.28 10:30 GMT
- <http://www.epa.gov/wastes/conserve/materials/textiles.htm>, US EPA. Retrieved 2015.04.12 20:40 GMT



- <http://nautilus.fis.uc.pt/st2.5/scenes-e/elem/e08230.html>, Applications of lead. Retrieved: 2014-08-01 10:00 GMT
- <http://www.usosof.net/uses-of-copper.html>, Uses of Copper. Retrieved 2014-08-01 10:00 GMT
- Huang F, Xu Y, Liao S, Yang D, Hsieh Y-L, Wei Q (2013) Preparation of amidoxime polyacrylonitrile chelating nanofibers and their application for adsorption of metal ions. *Materials* 3:969–980
- Imran A (2010) The quest for active carbon adsorbent substitutes: inexpensive adsorbents for toxic metal ions removal from wastewater. *Sep Purif Rev* 39:95–171
- Imran A (2012a) New generation adsorbents for water treatment. *Chem Rev* 112:5073–5091
- Imran A (2012b) Low cost adsorbents for the removal of organic pollutants from wastewater. *J Environ Manag* 113:170–183
- Imran A (2014) Water treatment by adsorption columns: evaluation at ground level. *Sep Purif Rev* 43:172–205
- Imran A, Gupta VK (2006) Advances in water treatment by adsorption technology. *Nat Protoc* 1:2661–2667
- IUPAC (1997) Compendium of chemical terminology. In: McNaught AD, Wilkinson A (eds) *The gold book*, 2nd edn. Blackwell Scientific Publications, Oxford
- Kaewsarn P, Yu QM (2001) Cadmium(II) removal from aqueous solutions by pre-treated biomass of marine alga *Padina* sp. *Environ Pollut* 2:209–213
- Kettle SFA, Tedder JM (1985) *The chemical bond*, 2nd edn. Wiley, New York
- Lagergren S (1898) Zur theorie der sogenannten adsorption gelöster stoffe. *Kungliga Svenska Vetenskapsakademiens. Handlingar* 4:1–39
- Langmuir I (1918) The adsorption of gases on plane surfaces of glass, mica and platinum. *J Am Chem Soc* 9:1361–1403
- Li L, Liu F, Jing X, Ling P, Li A (2011) Displacement mechanism of binary competitive adsorption for aqueous divalent metal ions onto a novel IDA-chelating resin: isotherm and kinetic modeling. *Water Res* 3:1177–1188
- Li Z, Kong Y, Ge Y (2015) Synthesis of porous lignin xanthate resin for Pb^{2+} removal from aqueous solution. *Chem Eng J* 270:229–234
- Liu C, Bai R, Ly QS (2008) Selective removal of copper and lead ions by diethylenetriamine-functionalized adsorbent: behaviors and mechanisms. *Water Res* 6–7:1511–1522
- Mao JA, Kwak IS, Sathishkumar M, Sneha K, Yun Y-S (2011) Preparation of PEI-coated bacterial biosorbent in water solution: optimization of manufacturing conditions using response surface methodology. *Bioresour Technol* 2:1462–1467
- Mitic-Stojanovic D-L, Zarubica A, Purenovic M, Bojic D, Andjelkovic T, Bojic Lj A (2011) Biosorptive removal of Pb^{2+} , Cd^{2+} and Zn^{2+} ions from water by *Lagenaria vulgaris* shell. *Water Sa* 3:303–312
- Muthu SS, Li Y, Hu J-Y, Mok P-Y (2012) Recyclability potential index (RPI): the concept and quantification of RPI for textile fibres. *Ecol Indic* 18:58–62
- Ngah WSW, Fatinathan S (2010) Pb(II) biosorption using chitosan and chitosan derivatives beads: equilibrium, ion exchange and mechanism studies. *J Environ Sci China* 3:338–346
- Nielen WFM, Marvin JPH (2008) *Comprehensive Analytical Chemistry*, 1st edn. Elsevier, Amsterdam
- Partington JR (1921) *A text-book of inorganic chemistry for university students*, 1st edn. Macmillan and co., London
- Pillai SS, Deepa B, Abraham E, Girija N, Geetha P, Jacob L, Koshy M (2013) Biosorption of Cd(II) from aqueous solution using xanthated nano banana cellulose: equilibrium and kinetic studies. *Ecotoxicol Environ Saf*. doi:10.1016/j.ecoenv.2013.09.003
- Pushpamalar V, Langford SJ, Ahmad M, Lim YY (2006) Optimization of reaction conditions for preparing carboxymethyl cellulose from sago waste. *Carbohydr Polym* 2:312–318
- Redlich O, Peterson DL (1959) A useful adsorption isotherm. *J Phys Chem* 63:1024
- Saleh TA (2011) The influence of treatment temperature on the acidity of MWCNT oxidized by HNO_3 or a mixture of HNO_3/H_2SO_4 . *Appl Surf Sci* 257:7746–7751
- Saleh TA (2015) Nanocomposite of carbon nanotubes/silica nanoparticles and their use for adsorption of Pb(II): from surface properties to sorption mechanism. *Desalin Water Treat*. doi:10.1080/19443994.2015.1036784
- Saleh TA, Gupta VK (2011) Functionalization of tungsten oxide into MWCNT and its application for sunlight-induced degradation of rhodamine B. *J Colloid Interface Sci* 362:337–344
- Saleh TA, Gupta VK (2012a) Synthesis and characterization of alumina nano-particles polyamide membrane with enhanced flux rejection performance. *Sep Purif Technol* 89:245–251
- Saleh TA, Gupta VK (2012b) Column with CNT/magnesium oxide composite for lead(II) removal from water. *Environ Sci Pollut Res* 19:1224–1228
- Saleh TA, Gupta VK (2014) Processing methods, characteristics and adsorption behavior of tire derived carbons: a review. *Adv Colloid Interface* 211:93–101
- Saleh TA, Agarwal S, Gupta VK (2011) Synthesis of MWCNT/MnO₂ and their application for simultaneous oxidation of arsenite and sorption of arsenate. *Appl Catal B Environ* 106:46–53
- Sheng PX, Ting Y-P, Chen JP (2007) Biosorption of heavy metal ions (Pb, Cu, and Cd) from aqueous solutions by the marine alga *Sargassum* sp. in single- and multiple-metal systems. *Ind Eng Chem Res* 8:2438–2444
- The National Academies of Sciences (1996) *Mineral resources and sustainability: challenges for earth scientists*. The National Academies Press, Washington, DC
- Tijssen CJ, Kolk HJ, Stamhuis EJ, Beenackers AACM (2001) An experimental study on the carboxymethylation of granular potato starch in non-aqueous media. *Carbohydr Polym* 3:219–226
- Won SW, Kotte P, Wei W, Lim A, Yun Y-S (2014) Biosorbents for recovery of precious metals. *Bioresour Technol*. doi:10.1016/j.biortech.2014.01.121
- Wu ZJ, Joo H, Lee K (2005) Kinetics and thermodynamics of the organic dye adsorption on the mesoporous hybrid xerogel. *Chem Eng J* 1–3:227–236
- Yang SP, Fu SY, Liu H, Zhou YM, Li XY (2011) Hydrogel beads based on carboxymethyl cellulose for removal heavy metal ions. *J Appl Polym Sci* 2:1204–1210

